Neurobiology of Disease 160 (2021) 105538

Contents lists available at ScienceDirect

Neurobiology of Disease

journal homepage: www.elsevier.com/locate/ynbdi

CXCR2 increases in ALS cortical neurons and its inhibition prevents motor neuron degeneration *in vitro* and improves neuromuscular function in SOD1G93A mice

Valentina La Cognata [a,1], Elisabetta Golini [b,1], Rosario Iemmolo [a], Sara Balletta [b], Giovanna Morello [a], Carla De Rosa [b], Ambra Villari [a], Sara Marinelli [b], Valentina Vacca [b], Gabriele Bonaventura [a], Paola Dell'Albani [a], Eleonora Aronica [c], Fabio Mammano [b,d], Silvia Mandillo [b,*], Sebastiano Cavallaro [a,*]

[a] Institute for Biomedical Research and Innovation, National Research Council, Via P. Gaifami 18, 95126 Catania, CT, Italy
[b] Institute of Biochemistry and Cell Biology, National Research Council, Via E. Ramarini 32, 00015 Monterotondo Scalo, RM, Italy
[c] Department of (Neuro) Pathology, Amsterdam UMC, University of Amsterdam, Amsterdam Neuroscience, Meibergdreef 9, 1105 Amsterdam, the Netherlands
[d] Department of Physics and Astronomy "G. Galilei", University of Padua, Padova, Italy

ARTICLE INFO

Keywords:
Amyotrophic lateral sclerosis
CXCR2
IL-8
iPSC
Motor neurons
Neurodegeneration
Reparixin
SOD1G93A mouse

ABSTRACT

Amyotrophic Lateral Sclerosis (ALS) is a progressive neurodegenerative disease characterized by depletion of motor neurons (MNs), for which effective medical treatments are still required. Previous transcriptomic analysis revealed the up-regulation of C-X-C motif chemokine receptor 2 (*CXCR2*)-mRNA in a subset of sporadic ALS patients and SOD1G93A mice. Here, we confirmed the increase of *CXCR2* in human ALS cortex, and showed that CXCR2 is mainly localized in cell bodies and axons of cortical neurons. We also investigated the effects of reparixin, an allosteric inhibitor of CXCR2, in degenerating human iPSC-derived MNs and SOD1G93A mice. *In vitro*, reparixin rescued MNs from apoptotic cell death, preserving neuronal morphology, mitochondrial membrane potential and cytoplasmic membrane integrity, whereas *in vivo* it improved neuromuscular function of SOD1G93A mice. Altogether, these data suggest a role for CXCR2 in ALS pathology and support its pharmacological inhibition as a candidate therapeutic strategy against ALS at least in a specific subgroup of patients.

1. Introduction

Amyotrophic lateral sclerosis (ALS) is a notoriously intractable neurodegenerative disorder involving specific loss of both upper and lower motor neurons (MNs). Approximately 10% of ALS cases are familial (FALS) and are mainly due to mutations occurring in *C9ORF72*, *SOD1*, *FUS* and *TDP-43* genes (Mathis et al., 2019), while the great majority are sporadic (SALS) and arise from multiple pathological drivers (e.g. oxidative stress, mitochondrial dysfunction, axonal transport alteration, inflammation, excitotoxicity and proteins aggregation) (van Es et al., 2017). Despite massive investments and intensive research in drug discovery, there is currently no available treatment to halt or reverse ALS. The only two approved drugs, riluzole and edaravone, exert limited effects in patients, whereas further pharmacologic agents which had seemed promising when tested in animal models, failed when translated into humans (Turner et al., 2001). These modest results may be due to both the poor knowledge of ALS pathophysiology and the use of animal models that do not faithfully reproduce the complexity and heterogeneity of the human disease (Bendotti et al., 2020).

We have recently used a genomic-based patient stratification (Aronica et al., 2015; Morello et al., 2017a) to portray sporadic ALS from a systems biology perspective and identify potential therapeutic targets

* Corresponding authors.
E-mail addresses: valentina.lacognata@cnr.it (V. La Cognata), elisabetta.golini@cnr.it (E. Golini), iemmolo.rosario@gmail.com (R. Iemmolo), balletta.sara@gmail.com (S. Balletta), giovanna.morello@irib.cnr.it (G. Morello), carla_derosa@outlook.com (C. De Rosa), ambra.villari@gmail.com (A. Villari), sara.marinelli@cnr.it (S. Marinelli), valentina.vacca@outlook.it (V. Vacca), gabriele.bonaventura@gmail.com (G. Bonaventura), paola.dellalbani@cnr.it (P. Dell'Albani), e.aronica@amsterdamumc.nl (E. Aronica), fabio.mammano@unipd.it (F. Mammano), silvia.mandillo@cnr.it (S. Mandillo), sebastiano.cavallaro@cnr.it (S. Cavallaro).
[1] Authors contributed equally.

https://doi.org/10.1016/j.nbd.2021.105538
Received 14 June 2021; Received in revised form 13 October 2021; Accepted 27 October 2021
Available online 29 October 2021

strategies (Lederer et al., 2007; Morello and Cavallaro, 2015; Morello et al., 2015; Morello et al., 2018; Morello et al., 2019; Morello et al., 2020). In particular, using transcriptional signatures of motor cortex samples, we discriminated control from sporadic ALS patients (SALS), and distinguished these latter into two greatly divergent subtypes (SALS1 and SALS2), each associated to different molecular features and potential drug targets (Aronica et al., 2015; Morello and Cavallaro, 2015; Morello et al., 2017b; La Cognata et al., 2020). Interestingly, some of these targets and related biological processes were shared by the SOD1G93A mice (Morello et al., 2017c), the most popular ALS animal model, thus providing a rationale starting point for their preclinical validation and the development of personalized treatments.

In this study we further investigated one of these potential targets, the C-X-C motif chemokine receptor 2 (CXCR2), which was previously found upregulated by transcriptomic analysis in a subset (SALS2) of ALS patients (Aronica et al., 2015) and in SOD1G93A mice at symptomatic stages (Morello et al., 2017a). This G-protein-coupled receptor is known for its main role of mediating neutrophils/monocytes chemotaxis and neuro-inflammatory response (De Paola et al., 2007; Won et al., 2016) through binding with at least seven C-X-C chemokines (Horuk et al., 1997; Nguyen and Stangel, 2001; Popivanova et al., 2003) and is involved in release of growth factors, chemotaxis of oligodendrocyte precursors during development, self-defense mechanisms against apoptotic cell death and modulation of synaptic transmission (Semple et al., 2010).

In order to understand the role of CXCR2 in ALS pathophysiology, in the present work we aimed to verify the expression of CXCR2 in human ALS cortex and investigate the effects of its pharmacological inhibition in degenerating human MNs derived from induced Pluripotent Stem Cells (iPSCs) and in SOD1G93A mice.

2. Methods

2.1. Motor cortex samples from SALS patients

Post-mortem frozen sections (thick 10 μm) of motor cortex samples of control, SALS1 and SALS2 patients (n = 3, 3 slides/patient) were obtained as described elsewhere (Aronica et al., 2015). Origin, source code, age, gender, race, disease state, survival time from diagnosis date and post-mortem interval of samples of patients used in the present study are reported in Suppl. Table 1.

For immunohistochemistry, slides were fixed with 4% paraformaldehyde (Thermo Fisher Scientific, Waltham, Massachusetts, USA) for 15 min, permeabilized with 0.1% of Triton-X for 10 min, washed 3× with phosphate-buffered saline (PBS) (Sigma Aldrich, Saint Louis, Missouri, USA) and stained with CXCR2 antibody (Suppl. Table 2) using EnVision™ Flex stain system according to manufacturer's instructions (Agilent Technologies, Santa Clara, California, USA). Sections were counterstained with Harris modified hematoxylin (Agilent Technologies, Santa Clara, California, USA) and mounted with crystal mount aqueous mounting medium (Sigma Aldrich, Saint Louis, Missouri, USA). Slides were examined under a Imager.D2 optical microscope through a 40× oil immersion lens (Carl Zeiss, Oberkochen, Germany). Representative photomicrographs were captured with an Axiovision Imaging System.

For immunofluorescence, fixed motor cortex slides were blocked and permeabilized with 5% normal goat serum (NGS), 0.1% of Triton-X in PBS for 45 min and incubated at room temperature with NF-H and CXCR2 primary antibodies (Suppl. Table 2). TRITC and FITC-conjugated secondary antibodies were used for 1 h at room temperature in dark. Tissues were washed 3× in PBS after every step. Slides were mounted with glycerol mounting medium containing 4′,6-diamidino-2-phenylindole (DAPI) and analyzed with a Nikon A1 confocal inverted microscope equipped with a Plan Apochromat lambda 60×/1.4 oil immersion lens (Nikon, Tokyo, Japan). Fluorescence was quantified by converting pixels in brightness values using the RGB normalized to the background as previously described (Inman et al., 2005).

2.2. Generation of iPSCs-derived MN and evaluation of reparixin effects

Reprogramming of human fibroblasts from a healthy donor subject into iPSCs was performed by transducting cells with Sendai Virus (SeV) vector harboring *OCT3/4, SOX2, KLF4,* and *c-MYC* in a feeder-free condition according to manufacturer's instructions (CytoTune-iPS kit, Life Technologies Corporation, Carlsbad, CA) (Suppl. Fig. S1). Tra1-60$^+$, Tra1-81$^+$ and OCT4$^+$ colonies were manually picked and transferred onto prepared vitronectin-coated well culture plates and checked for virus-free (Suppl. Fig. S1). MNs differentiation was performed as previously described (Hu and Zhang, 2009; Bonaventura et al., 2018; Bonaventura et al., 2021) (Suppl. Fig. S1). Differentiating medium lacked CXCR2 ligands and contained DMEM/F12, N2, MEM non-essential amino acids, heparin, BDNF, GDNF, IGF1, cAMP, ascorbic acid, retinoic acid and SHH.

For characterization, cells were fixed with 4% PFA for 15 min, permeabilized with 0.1% TRITON-X in PBS for 10 min and incubated overnight at 4 °C with anti-TUJ1, anti-SMI32, anti-ChAT, anti-CXCR2, anti-HB9 primary antibodies (Suppl. Table 2). TRITC and FITC-conjugated secondary antibodies were used for 1 h at room temperature in dark. Coverslips were then washed 3× in PBS, mounted with glycerol mounting medium containing DAPI on glass microscope slides, and analyzed with Nikon A1 confocal inverted microscope equipped with a Plan Apochromat lambda 60×/1.4 oil immersion lens (Nikon, Tokyo, Japan).

MTT cell viability experiments were conducted as previously described (Dell'Albani et al., 2017) in differentiated MNs cultured in complete medium (CTRL), growth factors starved medium, (-GF; without BDNF, GDNF, IGF1 and cAMP), and in -GF with the addition of reparixin (MedChem Express, NJ, USA) in order to characterize the maximum effective dose *in vitro*. This dose (10 μM for 48 h) was used in following assays to verify the pharmacological effects of reparixin on apoptosis, cellular morphology and mitochondrial membrane potential.

Apoptosis was determined by double-staining with Click-iT™ TUNEL Alexa Fluor™ 488 Imaging assay (Thermo Fisher Scientific, Waltham, Massachusetts, USA) and anti-TUJ1 primary antibody (Suppl. Table 2). Apoptotic cells were calculated by counting cells with NIS-Elements AR v4.60 software (Nikon, Tokyo, Japan) as follows: AI = number of apoptotic cells (TUNEL$^+$ nuclei)/total cell number (DAPI$^+$ nuclei) *100.

Neurite extensions were measured from ten fluorescent images of Tuj1 immunoreactivity from all experimental conditions, randomly acquired with Nikon Ti-Eclipse inverted microscope (Nikon, Tokyo, Japan) and using the "Annotations and Measurements" command of NIS-Elements software (Nikon, Tokyo, Japan).

Mitotoxicity and cytotoxicity levels were detected with the HCS Mitochondrial Health Kit (Thermo Fisher Scientific, Waltham, Massachusetts, USA) according to manufacture instructions. The MitoHealth stain accumulates in mitochondria in live cells proportional to the mitochondrial membrane potential, while the Image-iT® DEAD Green™ stain forms highly fluorescent dye-DNA complexes when plasma membrane integrity is compromised. Cells were scanned with a Nikon Ti-Eclipse inverted microscope through a Plan Fluor 20×/0.50 lens (Nikon, Tokyo, Japan) and acquired with NIS-Elements AR v4.60 software (Nikon, Tokyo, Japan). The fluorescence of different stains was quantified by converting pixels in brightness values using the RGB (green and red) normalized to the background as previously described (Inman et al., 2005).

2.3. Quantitative reverse-transcriptase polymerase chain reaction

RNA from motor cortex samples, iPSCs and differentiated MNs was isolated using TRIzol reagent (Thermo Fisher Scientific, Waltham, Massachusetts, USA) according to the manufacturer's instructions, as described elsewhere (D'Agata et al., 2002; Aronica et al., 2015).

Quantity and purity (260/280 and 260/230 ratios) of samples were determined using NanoDrop 1000 spectrophotometer (Thermo Fisher Scientific, Waltham, Massachusetts, USA) and Bioanalyzer RNA 6000 Nano chips (Agilent Technologies, Santa Clara, CA) as recommended by manufacturer. RNA was reverse transcribed with SuperScript™ III Reverse Transcriptase Kit (Thermo Fisher Scientific, Waltham, Massachusetts, USA) as previously described (Cavallaro et al., 2004). cDNA samples were used as template for RT-qPCR assays. Each reaction was run in triplicate and included 100 ng of cDNA, 4 μl of LightCycler® FastStart DNA Master SYBR Green I Plus (Roche Diagnostics, Monza, Italy), forward and reverse primers (250 nM), in a final volume reaction of 20 μl. All used primer pairs are listed in Suppl. Table 3. PCR conditions were set as follow: 1 cycle at 95 °C x 10 min; 45 cycles at 95 °C x 10 s, 55 °C x 15 s, 72 °C x 20 s and finally a single cycle at 65 °C x 1 min and 40 °C x 30 s. Gene expression profiles were evaluated by using the 2^ΔCq normalized with the housekeeping gene as previously reported (Taylor et al., 2019).

2.4. Reparixin administration to SOD1G93A mice and evaluation of its effects

Male B6.Cg-Tg(SOD1*G93A)1Gur/J mice (SOD1G93A) carrying a high copy number of mutant human SOD1 allele were purchased at the Jackson Laboratories (Bar Harbor, ME, USA, stock n. 004435) (Gurney et al., 1994) and a mouse colony was established in-house at the CNR-EMMA facility (Monterotondo, Italy) by crossing hemizygous transgenic males with C57BL/6 J females. Progeny was genotyped by standard PCR following the Jackson Lab protocol (www.jax.org).

Litter- and sex-matched pups were group-housed in standard housing conditions (room temperature 21 ± 2 °C, relative humidity 50–60%, and 12 h light/dark cycle with lights on at 7 am). Animals were subjected to experimental protocols approved by the Local Animal Welfare Committee and the Veterinary Dept. of the Italian Ministry of Health (Aut. #914/2016-PR), and experiments were conducted according to the ethical and safety rules and guidelines for the use of animals in biomedical research provided by the relevant Italian laws and European Union's directives (Italian Legislative Decree 26/2014 and 2010/63/EU). All adequate measures were taken to minimize animal pain or discomfort. Extra wet food was provided inside the cage as needed.

Male and female mice, SOD1G93A and non-transgenic (WT) littermates (males, $n = 29$/genotype, females $n = 32$/genotype) were submitted from the age of 6 weeks to specific behavioral tests to evaluate the onset and progression of ALS symptoms: body weight decline, neuromuscular deficits (grid hanging and grip strength tests), splay reflex and survival (age at humane endpoint). To evaluate the effects of a prolonged anti-inflammatory treatment, male and female, SOD1G93A and WT mice were randomly assigned to treatment groups as described in the Statistical analysis section. Mice were injected i.p. with either 30 or 60 mg/kg reparixin L-lysine salt (MedChemTronica, Sollentuna, Sweden). Control group mice were administered saline (0.9% NaCl). Mice were injected 2 times/week from the age of 14 weeks (ca. 100 days, initial symptomatic stage) until humane endpoint. Behavioral tests were conducted during the course of the disease until SOD1G93A mice were no longer able to perform the task. Experimenters performing behavioral tests were blind to the treatment groups but not to the genotype since specific symptoms were clearly visible in SOD1G93A mice.

2.4.1. Body weight, symptoms and humane endpoint assessment

Body weight (BW) was measured weekly from age 6 weeks and after each behavioral test. Body weight gain was calculated and data were expressed as percentage variation of weight compared to the first measure taken at 6 weeks of age. Monitoring of disease symptoms was achieved by direct observation and annotation of tremors, splay reflex loss, bradykinesia and paralysis (Deitch et al., 2014). Disease onset was set at age of splay reflex loss and peak body weight (Melanie Leitner and Lutz, 2009). Humane endpoint was set at loss of righting reflex or weight loss >25% of peak BW. Age (days) at humane endpoint was used to perform survival analysis.

2.4.2. Grid hanging test

Mice were tested weekly from the age of 6 weeks. Each mouse was placed in the center of a wire grid (1-cm squares) raised about 50 cm from a bench covered with sawdust bags and forced to grip it by gentle shaking. After rotating the grid upside down the latency to fall from the grid was recorded over two trials of 60 s each, with an inter-trial interval of approx. 30 min (Weydt et al., 2003; OlivÁN et al., 2015). For each time point the total time of the two trials was considered in the analysis.

2.4.3. Grip strength test

Mice were tested on the grip strength meter apparatus (Bioseb, France) every two weeks from the age of 7 weeks until 21 weeks. Each mouse was held gently by the base of its tail over the top of the grid with its torso in a horizontal position, then it was pulled back steadily until it could no longer resist the increasing force and the grip was released (Mandillo et al., 2008). The grip strength meter digitally displays the maximum force applied as the peak tension (in grams) once the grasp is released. For each mouse the grip test consisted of three trials with forelimbs and three trials with all four paws with an inter-trial interval of 60 s. For each time point the mean of the three trials was taken as an index of forelimb and all four paws grip strength.

2.5. Statistical analysis

For *in vitro* experiments, one-way analysis of variance (ANOVA) was used to compare differences among groups, and statistical significance was assessed by the *Tukey–Kramer* post hoc test. In the *in vivo* experiments, estimated sample size ($n = 10$/group) was determined by power analysis (G*Power 3.1). Male and female, SOD1G93A and WT mice were randomly assigned to the three treatment groups so that all cage-mates received the same treatment and, in case of litters split among multiple cages, the mice of the same litter were homogeneously distributed to different treatment groups. Repeated measures ANOVA (RM ANOVA) was performed on most datasets with Genotype, Sex and Treatment as between-subject factors and Age as within-subject factors. For each behavioral test repeated-measures analyses were performed until an age at which data were available for all animals (19–20 weeks of age depending on test). *Post-hoc* analysis (Bonferroni test) was performed where possible. Survival and time to 20% decline of grid hanging endurance of SOD1G93A mice were represented with Kaplan-Meier curves and were analyzed using a Log-rank (Mantel-Cox) test followed by corrected multiple comparisons using Gehan-Breslow-Wilcoxon test. Mean ± SEM of survival days was also used to assess survival differences and analyzed with one-way analysis of variance. Subjects whose individual values differed more than 2 standard deviation units in module from the group average were considered outliers and were excluded from the analysis. Significance level was set at $P < 0.05$. Data are presented as mean ± SEM. All statistics were run using the StatView 5.0 PowerPC and Prism 5.0a (GraphPad Software Inc., La Jolla, CA, USA) software packages.

3. Results

3.1. CXCR2 mRNA and its encoded protein are up-regulated in motor cortex of SALS2 patients

In our previous work, whole-genome transcriptional profiling of human SALS motor cortex revealed a significant up-regulation of *CXCR2*-mRNA in a subgroup of patients (SALS2) (Aronica et al., 2015). To corroborate these data, we measured *CXCR2*-mRNA by RT-qPCR ($n = 3$/group) and confirmed the increased expression levels in SALS2 cortex compared to both control and SALS1 (ANOVA: $F_{(2, 6)} = 391.9$, $p < 0.0001$; Fig. 1a). Immunohistochemistry and immunofluorescence

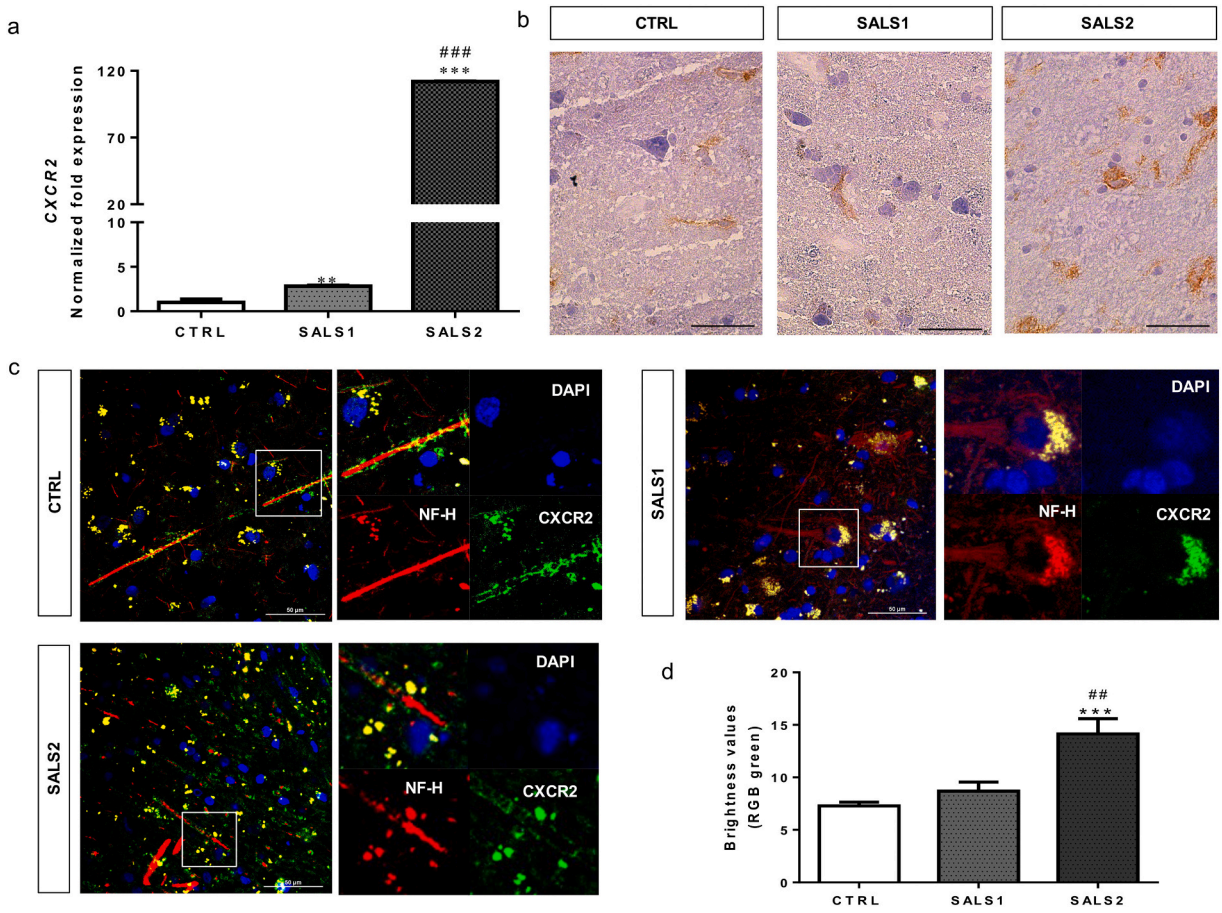

Fig. 1. CXCR2 is up-regulated in motor cortex of SALS2 patients and is localized in cortical neurons.
a) RT-qPCR assay showing a statistically significant up-regulation of CXCR2 gene expression in SALS2 compared to both SALS1 and CTRL groups ($n = 3$ per group). Data are normalized with the amount of β-actin mRNA, and are expressed as mean ± SEM. Tukey–Kramer post hoc test: *** and ### $p < 0.001$ SALS2 vs CTRL and SALS1 respectively, ** $p < 0.01$ SALS1 vs CTRL.
b) Representative photomicrographs showing CXCR2 immunoreactivity in motor cortex samples of normal subjects, SALS1 and SALS2 patients examined under a light microscope (Axiovert, Carl Zeiss Inc) equipped with a digital color camera. Scale bar 50 μm.
c) Representative photomicrographs showing CXCR2 immunoreactivity in motor cortex samples of CTRL, SALS1 and SALS2 subjects examined with a Nikon A1 confocal inverted microscope equipped with a Plan Apochromat lambda 60×/1.4 oil immersion lens. Scale bar 50 μm. Zoom-in with distinct channels are provided.
d) Brightness intensity of CXCR2 immunoreactivity from motor cortex samples of CTRL, SALS1 and SALS2 patients (n = 3/group). Brightness values were calculated as described in Materials and methods section and expressed as mean ± SEM. Tukey–Kramer post hoc test: ***$p < 0.001$ SALS2 vs CTRL; $^{\#\#}p < 0.01$ SALS2 vs SALS1.

experiments (Fig. 1b, c) detailed the expression of CXCR2 protein in human motor cortex, revealing its localization in cell bodies and axons of cortical neurons (pyramidal cells in layer V) and a significant increase in SALS2 patients compared to both control and SALS1 (ANOVA: $F_{(2, 24)} = 13.27$, $p = 0.0001$; Fig. 1d).

3.2. CXCR2 inhibition by reparixin preserves human iPSC-derived MNs from degeneration

To investigate the pharmacological effects of CXCR2 inhibition *in vitro*, we examined the effects of reparixin, an allosteric inhibitor of CXCR2, in degenerating human MNs-like cells derived from iPSC reprogramming and motor neuronal induction (Suppl. Fig. S1) (Hu and Zhang, 2009; Bonaventura et al., 2018). Once differentiated, cells expressed mature MN biomarkers (SMI32, ChAT, HB9 and Tuj1), CXCR2 (Fig. 2a) and its main ligand IL-8 (Suppl. Fig. 2). Deprivation of growth factors from culture medium (-GF condition) for 48 h determined an increase of both mRNA and protein IL-8 levels (Suppl. Fig. 2) and prompted neuronal death (Fig. 2b). The simultaneous administration of 10 μM reparixin significantly preserved cellular viability (ANOVA: $F_{(2,27)} = 68.33$, $p \leq 0.0001$; Fig. 2b), reduced MN apoptosis (calculated as the percentage of $Tuj1^+/TUNEL^+$ cells; ANOVA: $F_{(2,12)} = 138.6$, $p < 0.0001$; Fig. 2c), and preserved neurites length (ANOVA: $F_{(2, 400)} = 49.88$, $p < 0.0001$; Fig. 2d). Moreover, by using both MitoHealth (which accumulates in mitochondria in live cells proportional to the mitochondrial membrane potential) and Image-iT DEAD Green (which penetrates inside cells when plasma membrane integrity is compromised) stains, we quantified mitotoxicity and cytotoxicity (Fig. 2e). Treatment with reparixin increased MitoHealth stain accumulation in mitochondria compared to -GF condition, and preserved the integrity of cytoplasmic membrane (ANOVA RGB MitoHealth stain: $F_{(2, 24)} = 11.18$, $p = 0.0004$; ANOVA RGB DEAD Green stain: $F_{(2, 24)} = 12.50$, $p = 0.0002$; Fig. 2e).

3.3. Reparixin reduces body weight loss and improves neuromuscular function in SOD1G93A mice

To investigate the pharmacological effects of CXCR2 inhibition *in vivo*, we examined the effects of reparixin in SOD1G93A mice. Male and female SOD1G93A mice and their WT littermates were monitored from 6 weeks of age until humane endpoint. From symptomatic stage (around 100 days, i.e. 14 weeks of age) mice were administered saline, 30 or 60 mg/kg reparixin 2/week until 21–24 weeks of age (humane endpoint). Body weight, neuromuscular function and symptoms were assessed

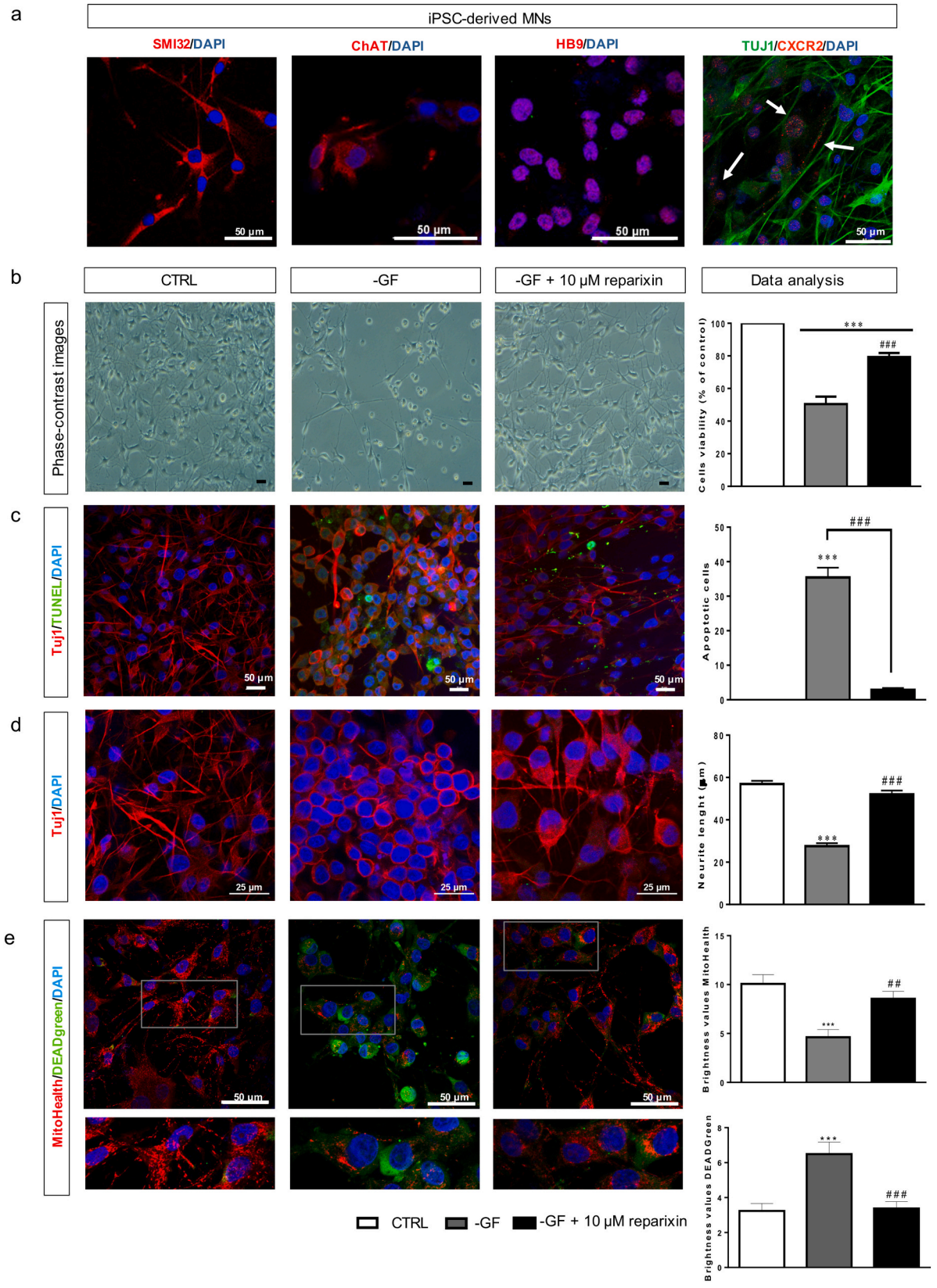

(caption on next page)

Fig. 2. Reparixin preserves cellular viability, neurites outgrowth, membrane integrity and reduces apoptosis of iPSC-derived MNs.
a) Immunocytochemistry experiments in differentiated MNs-like cells at 35th day showing the expression of Tuj1, SMI32, and ChAT, HB9 and CXCR2 (white arrows). Nuclei were counterstained with DAPI. Photomicrographs are representative of randomly selected fields and scanned by Nikon Ti Eclipse inverted microscope. Scale bar 50 μm.
b) Representative phase-contrast photomicrographs and MTT viability analysis of iPSC-derived MNs cultured in complete growth medium (CTRL), growth factor starved medium (-GF) or -GF + 10 μM reparixin. Scale bar 50 μm. Data are expressed as percentage of control (mean ± SEM) and are representative of at least three independent experiments. Tukey–Kramer post hoc test: ***$p < 0.001$ vs Ctrl; $^{###}p < 0.001$ vs -GF.
c) Apoptotic counting by TUNEL assay of iPSC-derived MNs cultured in complete (CTRL), -GF or -GF + 10 μM reparixin medium. Photomicrographs are representative of randomly selected fields and were scanned by Nikon Ti Eclipse inverted microscope. Scale bar 50 μm. Data are representative of at least three independent experiments. The apoptotic index was calculated as described in Material and Methods Section and is expressed as mean ± SEM. Tukey–Kramer post hoc test: ***$p < 0.001$ vs Ctrl; $^{###}p < 0.001$ vs -GF.
d) Effects of growth factors starvation and reparixin treatment on neurites outgrowth. Representative cropped photomicrographs showing Tuj1 immunoreactivity in human iPSC-derived MNs cultured in complete (CTRL), -GF or -GF + 10 μM reparixin medium. Representative results are taken from randomly selected fields of slides scanned by a Nikon Ti Eclipse inverted microscope (scale bar 25 μm). Neurite length (in micron) was evaluated with NIS Elements software and is represented as mean ± SEM. Data are representative of three independent experiments. Tukey–Kramer post hoc test: ***$p < 0.001$ vs Ctrl; $^{###}p < 0.001$ vs -GF.
e) Representative photomicrographs of human iPSC-derived MNs cultured in complete (CTRL), -GF or -GF + 10 μM reparixin medium stained with HCS kit. Representative results were taken from randomly selected fields of slides scanned by a Nikon Ti Eclipse inverted microscope (scale bar 50 μm). Brightness values (mean ± SEM) were calculated as described in Material and Methods Section. Tukey–Kramer post hoc test: ***$p < 0.001$ vs Ctrl; $^{###}p < 0.001$ vs –GF, $^{##}p < 0.01$ vs –GF.

throughout the experiment (Fig. 3a). As expected, body weight of both male and female control SOD1G93A mice started declining around 17 weeks of age, reflecting a reduction in muscular mass. In particular, body weight and grip strength in the transgenic mice differed significantly from WT littermates earlier in males than in females (Suppl. Fig. S3a, b). Treatment with reparixin from age 14 weeks elicited a significant effect in reducing the % body weight loss at endpoint only in female SOD1G93A mice and in a dose dependent fashion (ANOVA: $F_{(2,28)} = 4.633$, $p = 0.0183$; Fig. 3b, c). Moreover, systemic administration of reparixin was able to improve neuromuscular function in SOD1G93A mice (Fig. 3d-g). This effect was clearly evident and dose dependent in the grid-hanging test (a measure of resistance) both in males (between 16 and 20 weeks of age; RM ANOVA: Treatment $F_{(2,51)} = 4.907$, $p = 0.01$; Genotype, $F_{(1,51)} = 144.163$, $p < 0.0001$; Treatment x Genotype, $F_{(2,51)} = 4.856$, $p = 0.01$; Fig. 3d) and females (from 17 until 22 weeks of age; RM ANOVA: Treatment, $F_{(2,57)} = 12.503$, $p < 0.0001$; Genotype, $F_{(1,57)} = 49.441$, $p < 0.0001$; Treatment x Genotype, $F_{(2,57)} = 12.503$, $p < 0.0001$; Fig. 3e). Interestingly, in SOD1G93A mice, the reparixin-induced improvement of neuromuscular resistance compared to the saline treated group was more effective in females at the highest dose, delaying the onset of motor deficit by about 4 weeks (Fig. 3e; Suppl. Fig. S3d). Similarly, reparixin administration affected the grip strength performance of SOD1G93A mice compared to WT littermates (RM ANOVA Males: Genotype x Treatment, $F_{(2,52)} = 3.196$, $p < 0.05$; Females: Genotype x Treatment, $F_{(2,57)} = 4.72$, $p = 0.012$; Fig. 3f, g). In this case, the highest dose of reparixin was effective only in females (Fig. 3g). With disease progression, the beneficial effect of reparixin on neuromuscular function was overcome by more severe symptoms and treatment was not able to increase the survival of SOD1G93A mice (Suppl. Fig. S3e, f).

4. Discussion

ALS is a progressive adult-onset neurodegenerative disease, always fatal. Although several studies have been granted to develop effective therapies against ALS, this remains a progressive and incurable disease. The only two approved treatments, riluzole and edaravone, exert partial benefits to patients, while other pharmacological agents, successfully tested in animal models, failed once translated into patients clinical trials (Turner et al., 2001).

In the present study we investigated CXCR2, a candidate pharmacological target that has been formerly observed deregulated by bulk transcriptomic profiling in both ALS human cortex and SOD1G93A mice (Morello et al., 2017b). This G-protein coupled receptor is expressed at low basal level in CNS (projections of cerebral cortex neurons, hippocampus, cerebellum and spinal cord motor neurons) (Horuk et al., 1997), and highly expressed peripherally in neutrophils (Walz et al., 1987), monocytes (Bonecchi et al., 2000), T-lymphocytes and mast cells (Nilsson et al., 1999; Lippert et al., 2004), fibroblasts (Nirodi et al., 2008) and endothelial cells (Strieter et al., 1995). This widespread and systemic CXCR2 expression correlates with its main biological role, which is mediating inflammatory mechanisms in response to endogenous ligands (Semple et al., 2010). Upon brain damage (infection, injury, lesions, amyloid plaques or other neuronal protein aggregates), CXCR2 ligands are produced by glial (activated microglia and astrocytes) and endothelial cells, inducing a high inflammatory state via neutrophils infiltration into the site of damage and contributing to neuronal degeneration (Semple et al., 2010; Ha et al., 2017).

Here we showed for the first time the expression of CXCR2 in human motor cortex specimens of control and SALS patients, describing its predominant localization in cell bodies and axons of cortical neurons. Moreover, we reported CXCR2 up-regulation at both transcriptional and protein levels in a subgroup of ALS patients (SALS2), a finding in accordance with the deregulation of a SALS2 cluster-specific gene set involving players of the immune/inflammatory pathways (Morello et al., 2017c). Interestingly, the up-regulation of CXCR2 has been observed in various other neuropathological conditions such as multiple sclerosis, ischemia, traumatic brain injury, and Alzheimer's disease (Semple et al., 2010; Veenstra and Ransohoff, 2012).

To test the pharmacological effects of CXCR2 inhibition in ALS, we administered an allosteric inhibitor of CXCR2 (reparixin) *in vitro*, in human degenerating iPSC-derived MNs, and *in vivo* in SOD1G93A mice. *In vitro*, reparixin prevented apoptotic neuronal death in iPSC-derived MNs ($Tuj1^+$, $HB9^+$, $SMI32^+$, $ChAT^+$, $CXCR2^+$) following growth-factors withdrawal, preserving neuronal morphology, mitochondrial membrane potential and cytoplasmic membrane integrity. IL-8 quantification experiments (by RT-qPCR and ELISA assays) revealed the main CXCR2-ligand is produced under control conditions and that its expression increases following growth factors withdrawal (Suppl. Fig. S2). Based on this evidence, the effect of reparixin *in vitro* may be related to the antagonism of autocrine/paracrine IL-8 activation of CXCR2.

In vivo (Gurney et al., 1994), repeated administration of reparixin was particularly effective in female SOD1G93A mice, where it delayed by four weeks the onset of neuromuscular decline and reduced body weight loss at endpoint. Sex differences observed may reflect differences in disease progression between males and females SOD1G93A mice. Indeed, reparixin treatment started in both sexes at 14 weeks of age, when females SOD1G93A mice display less evident symptoms compared to males (Alves et al., 2011; Cervetto et al., 2013; Oliván et al., 2014). The exact mechanisms of action underlying reparixin protective effects *in vivo*, as well as the role of non-neuronal cell in mediating inflammatory response need further investigations. Additional studies are necessary to characterize the effects of reparixin on neuronal viability,

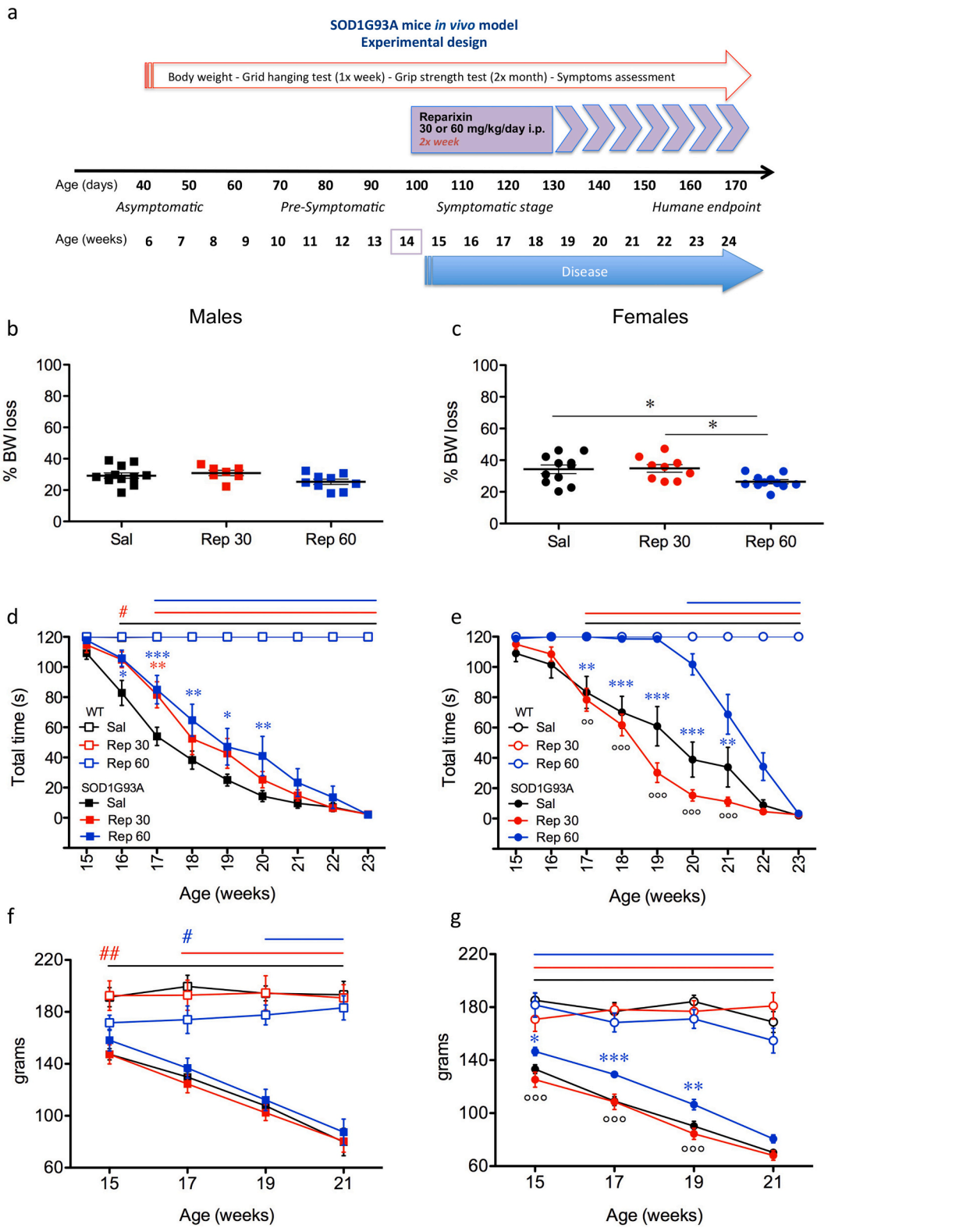

(caption on next page)

Fig. 3. Reparixin treatment effects on body weight loss and neuromuscular function of SOD1G93A mice.
a) Experimental design. Time line of behavioral tests and treatment with reparixin from age 14 weeks to endpoint.
b-c) Percentage body weight loss calculated at humane endpoint for male (b) and female (c) SOD1G93A mice of Sal, Rep30, Rep60 groups. Dot plots and line are mean ± SEM. Tukey's post hoc: *$p < 0.05$. Males: Sal $n = 12$; Rep30: $n = 7$; Rep60: $n = 9$. Females: Sal $n = 11$; Rep30: n = 9; Rep60: $n = 11$. d-e) Latency to fall (seconds, mean ± SEM) of male (d) and female (e) mice in the grid hanging test after reparixin treatment. Pre-treatment data are not shown since all mice reached the maximum latency 120 s. Bonferroni post hoc's: Red # $p < 0.05$, color lines $p < 0.001$, WT vs. SOD1G93A within respective treatment groups at specific time points. In SOD1G93A mice, red **$p < 0.01$, Sal vs. Rep30; blue *$p < 0.05$, **$p < 0.01$, ***$p < 0.001$ Sal vs. Rep60, black °°$p < 0.01$, °°°$p < 0.001$ Rep30 vs. Rep60. Males: Sal (WT, n = 12; SOD1G93A, n = 11), Rep30 (WT, $n = 8$; SOD1G93A, n = 7) or Rep60 (WT, n = 9; SOD1G93A, $n = 10$). Females: Sal (WT, n = 11; SOD1G93A, n = 11), Rep30 (WT, n = 9; SOD1G93A, n = 8) or Rep60 (WT, n = 12; SOD1G93A, n = 12). f-g) Grip strength (4-paws force) of male (f) and female (g) WT and SOD1G93A mice measured bi-monthly from 15 to 21 weeks of age after the injection of either Sal, Rep30 or Rep60. Line colors and symbols are the same as in Panels d-e. Bonferroni post hocs: lines on top indicate $p < 0.001$ WT vs. SOD1G93A mice of respective treatment groups at specific time points; blue #$p < 0.05$ WT vs. SOD1G93A in Rep60 group; red ##$p < 0.01$ WT vs. SOD1G93A in Rep30 group.; In SOD1G93A mice: Blue *$p < 0.05$; **$p < 0.01$; ***$p < 0.001$ Rep60 vs. Sal; Black °°°$p < 0.001$ Rep30 vs. Rep60. Males: Sal (WT, n = 12; SOD1G93A, n = 12), Rep30 (WT, n = 8; SOD1G93A, n = 7) or Rep60 (WT, n = 9; SOD1G93A, n = 10). Females: Sal (WT, n = 11; SOD1G93A, n = 11), Rep30 (WT, n = 9; SOD1G93A, n = 8) or Rep60 (WT, n = 12; SOD1G93A, n = 12).

apoptosis and morphology. It is noteworthy that systemic administration of reparixin at doses similar to those used in the present study produces significant effects in models of other CNS pathologies, as shown in models of cerebral ischemia (Garau et al., 2005; Villa et al., 2007; Sousa et al., 2013), cerebral hemorrhage (Matsushita et al., 2014), spinal cord injury (Gorio et al., 2007; Marsh and Flemming, 2011), and low back pain (Krock et al., 2019).

Although a single *in vitro* study has previously reported some beneficial effects of reparixin in rodent-based motor neuronal primary cultures (De Paola et al., 2007), this is the first evidence in human iPSC-derived MNs and in a ALS animal model. The effects of reparixin in SOD1G93A mice are remarkable when compared to riluzole and edaravone (Jaiswal, 2018). Riluzole administration improves SOD1G93A mice lifespan (Gurney et al., 1996) but has no effect on motor functions (Raoul et al., 2013; Hogg et al., 2017), while edaravone slows motor decline and body weight loss by 4–11 days in female SOD1G93A mice but does not significantly increase survival (Ito et al., 2008).

Further studies are still required to fully elucidate the role of CXCR2 in ALS pathogenesis, to define the most appropriate doses, timing or route of administration of reparixin and, most importantly, to allow proper translation from animal models to humans. To this regard, we found deregulated *SOD1* expression in SALS2 patients (Aronica et al., 2015; Morello et al., 2017a), suggesting that the SOD1G93A mice may represent a well-suited preclinical model to investigate SALS2 pathology.

In conclusion, our findings suggest CXCR2 as a candidate therapeutic target for ALS at least in a specific subgroup of patients. Furthermore, our data highlight that genomic stratification of ALS patients, together with the appropriate selection and prioritization of potential drug targets, may represent a promising strategy to rationally design and develop patient-tailored target therapies.

List of abbreviations

ALS	Amyotrophic Lateral Sclerosis
BW	Body weight
ChAT	Choline *O*-acetyltransferase
CXCR2	C-X-C motif chemokine receptor 2
DAPI	4′,6-diamidino-2-phenylindole
FALS	Familiar Amyotrophic Lateral Sclerosis
HB9	Homeobox HB9 (HLXB9)
iPSC	induced Pluripotent Stem Cells
MNs	Motor neurons
NGS	Normal Goat Serum
PBS	Phosphate-buffered saline
PFA	paraformaldehyde
SALS	Sporadic Amyotrophic Lateral Sclerosis
SALS1	Sporadic Amyotrophic Lateral Sclerosis subgroup 1
SALS2	Sporadic Amyotrophic Lateral Sclerosis subgroup 2
SEM	standard error of mean
SMI32	Small Integral Membrane Protein 32
TuJ1	Neuron-specific class III beta-tubulin

Ethics approval and consent to participate

Informed consent was obtained for the use of brain tissue and for access to medical records for research purposes and approval was obtained from the relevant local ethical committees for medical research as previously reported (Aronica et al., 2015). Experiments with human cells were approved by an ethical committee for medical research from "Vittorio Emanuele" University Hospital in Catania (Approval No. 17239) and performed in accordance with ethical standards. Animal experiments were subjected to experimental protocols approved by the Local Animal Welfare Committee and the Veterinary Dept. of the Italian Ministry of Health (Aut. #914/2016-PR), and experiments were conducted according to the ethical and safety rules and guidelines for the use of animals in biomedical research provided by the relevant Italian laws and European Union's directives (Italian Legislative Decree 26/2014 and 2010/63/EU).

Consent to publication

Consent for publication of images and data was obtained from patients.

Availability of data and materials

Transcriptional data are available at EBI ArrayExpress database with the accession number E-MTAB-2325 (https://www.ebi.ac.uk/arrayexpress/experiments/E-MTAB-2325/).

Funding

The work at IRIB was supported by grants i) "Development and application of biosensoristic technologies in genomics" by European Social Fund operational program for the Sicily region (Italy), PO FESR Sicily 2014–2020 (CIP 2014.IT.05.SFOP.014/3/10.4/9.2.10/0008) and ii) "Flagship Project InterOmics - Cell-based Omics for research applications in precision medicine" by National Research Council – CNR. The work at IBBC was supported by Infrafrontier-I3 project under EU contract Grant Agreement Number 312325 of the EC FP7; Project of strategic interest "Aging" from National Research Council – CNR.

Declaration of Competing Interest

The authors declare that the research was conducted in the absence of any commercial or financial relationships that could be construed as a potential conflict of interest.

Acknowledgments

Authors gratefully acknowledge Cristina Calì, Alfia Corsino, Maria

Patrizia D'Angelo and Francesco Marino for administrative and technical support. We also thank Simone Gozzi, Giampaolo D'Erasmo, Simone Manghisi and Alessandro Grop for excellent animal care support. We are grateful to the International Mouse Phenotyping Consortium (IMPC) for fruitful sharing of procedures and discussions.

Appendix A. Supplementary data

Supplementary data to this article can be found online at https://doi.org/10.1016/j.nbd.2021.105538.

References

Alves, C.J., de Santana, L.P., Santos, A.J.D.D., de Oliveira, G.P., Duobles, T., Scorisa, J. M., Martins, R.S., Maximino, J.R., Chadi, G., 2011. Early motor and electrophysiological changes in transgenic mouse model of amyotrophic lateral sclerosis and gender differences on clinical outcome. Brain Res. 1394, 90–104. https://doi.org/10.1016/j.brainres.2011.02.060.

Aronica, E., Baas, F., Iyer, A., ten Asbroek, A.L., Morello, G., Cavallaro, S., 2015. Molecular classification of amyotrophic lateral sclerosis by unsupervised clustering of gene expression in motor cortex. Neurobiol. Dis. 74, 359–376. https://doi.org/10.1016/j.nbd.2014.12.002.

Bendotti, C., Bonetto, V., Pupillo, E., Logroscino, G., Al-Chalabi, A., Lunetta, C., Riva, N., Mora, G., Lauria, G., Weishaupt, J.H., Agosta, F., Malaspina, A., Basso, M., Greensmith, L., Van Den Bosch, L., Ratti, A., Corbo, M., Hardiman, O., Chiò, A., Silani, V., Beghi, E., 2020. Focus on the heterogeneity of amyotrophic lateral sclerosis. In: Amyotrophic Lateral Sclerosis and Frontotemporal Degeneration, pp. 1–11. https://doi.org/10.1080/21678421.2020.1779298.

Bonaventura, G., Iemmolo, R., D'Amico, A.G., La Cognata, V., Costanzo, E., Zappia, M., D'Agata, V., Conforti, F.L., Aronica, E., Cavallaro, S., 2018. PACAP and PAC1R are differentially expressed in motor cortex of amyotrophic lateral sclerosis patients and support survival of iPSC-derived motor neurons. J. Cell. Physiol. 233 (4), 3343–3351. https://doi.org/10.1002/jcp.26182.

Bonaventura, G., Iemmolo, R., Attaguile, G.A., La Cognata, V., Pistone, B.S., Raudino, G., D'Agata, V., Cantarella, G., Barcellona, M.L., Cavallaro, S., 2021. iPSCs: a preclinical drug research tool for neurological disorders. Int. J. Mol. Sci. 22 (9) https://doi.org/10.3390/ijms22094596.

Bonecchi, R., Facchetti, F., Dusi, S., Luini, W., Lissandrini, D., Simmelink, M., Locati, M., Bernasconi, S., Allavena, P., Brandt, E., Rossi, F., Mantovani, A., Sozzani, S., 2000. Induction of functional IL-8 receptors by IL-4 and IL-13 in human monocytes. J. Immunol. 164 (7), 3862–3869. https://doi.org/10.4049/jimmunol.164.7.3862.

Cavallaro, S., D'Agata, V., Alessi, E., Coffa, S., Alkon, D.L., Manickam, P., Ciotti, M.T., Possenti, R., Bonini, P., Marlier, L., Calissano, P., 2004. Gene expression profiles of apoptotic neurons. Genomics 84 (3), 485–496. https://doi.org/10.1016/j.ygeno.2004.04.006.

Cervetto, C., Frattaroli, D., Maura, G., Marcoli, M., 2013. Motor neuron dysfunction in a mouse model of ALS: gender-dependent effect of P2X7 antagonism. Toxicology 311 (1–2), 69–77. https://doi.org/10.1016/j.tox.2013.04.004.

D'Agata, V., Zhao, W., Pascale, A., Zohar, O., Scapagnini, G., Cavallaro, S., 2002. Distribution of parkin in the adult rat brain. Prog. Neuro-Psychopharmacol. Biol. Psychiatry 26 (3), 519–527.

De Paola, M., Buanne, P., Biordi, L., Bertini, R., Ghezzi, P., Mennini, T., 2007. Chemokine MIP-2/CXCL2, acting on CXCR2, induces motor neuron death in primary cultures. Neuroimmunomodulation 14 (6), 310–316. https://doi.org/10.1159/000123834.

Deitch, J.S., Alexander, G.M., Bensinger, A., Yang, S., Jiang, J.T., Heiman-Patterson, T. D., 2014. Phenotype of transgenic mice carrying a very low copy number of the mutant human G93A superoxide dismutase-1 gene associated with amyotrophic lateral sclerosis. PLoS One 9 (6), e99879. https://doi.org/10.1371/journal.pone.0099879.

Dell'Albani, P., Di Marco, B., Grasso, S., Rocco, C., Foti, M.C., 2017. Quercetin derivatives as potent inducers of selective cytotoxicity in glioma cells. Eur. J. Pharm. Sci. 101, 56–65. https://doi.org/10.1016/j.ejps.2017.01.036.

Garau, A., Bertini, R., Colotta, F., Casilli, F., Bigini, P., Cagnotto, A., Mennini, T., Ghezzi, P., Villa, P., 2005. Neuroprotection with the CXCL8 inhibitor repertaxin in transient brain ischemia. Cytokine 30 (3), 125–131. https://doi.org/10.1016/j.cyto.2004.12.014.

Gorio, A., Madaschi, L., Zadra, G., Marfia, G., Cavalieri, B., Bertini, R., Di Giulio, A.M., 2007. Reparixin, an inhibitor of CXCR2 function, attenuates inflammatory responses and promotes recovery of function after traumatic lesion to the spinal cord. J. Pharmacol. Exp. Ther. 322 (3), 973–981. https://doi.org/10.1124/jpet.107.123679.

Gurney, M., Pu, H., Chiu, A., Dal Canto, M., Polchow, C., Alexander, D., Caliendo, J., Hentati, A., Kwon, Y., Deng, H., et al., 1994. Motor neuron degeneration in mice that express a human Cu,Zn superoxide dismutase mutation. Science 264 (5166), 1772–1775. https://doi.org/10.1126/science.8209258.

Gurney, M.E., Cutting, F.B., Zhai, P., Doble, A., Taylor, C.P., Andrus, P.K., Hall, E.D., 1996. Benefit of vitamin E, riluzole, and gababapentin in a transgenic model of familial amyotrophic lateral sclerosis. Ann. Neurol. 39 (2), 147–157. https://doi.org/10.1002/ana.410390203.

Ha, H., Debnath, B., Neamati, N., 2017. Role of the CXCL8-CXCR1/2 Axis in cancer and inflammatory diseases. Theranostics 7 (6), 1543–1588. https://doi.org/10.7150/thno.15625.

Hogg, M.C., Halang, L., Woods, I., Coughlan, K.S., Prehn, J.H.M., 2017. Riluzole does not improve lifespan or motor function in three ALS mouse models. Amyotr. Lat. Scler. Frontotemp. Degen. 19 (5–6), 438–445. https://doi.org/10.1080/21678421.2017.1407796.

Horuk, R., Martin, A.W., Wang, Z., Schweitzer, L., Gerassimides, A., Guo, H., Lu, Z., Hesselgesser, J., Perez, H.D., Kim, J., Parker, J., Hadley, T.J., Peiper, S.C., 1997. Expression of chemokine receptors by subsets of neurons in the central nervous system. J. Immunol. 158 (6), 2882–2890.

Hu, B.Y., Zhang, S.C., 2009. Differentiation of spinal motor neurons from pluripotent human stem cells. Nat. Protoc. 4 (9), 1295–1304. https://doi.org/10.1038/nprot.2009.127.

Inman, C.F., Rees, L.E., Barker, E., Haverson, K., Stokes, C.R., Bailey, M., 2005. Validation of computer-assisted, pixel-based analysis of multiple-colour immunofluorescence histology. J. Immunol. Methods 302 (1–2), 156–167. https://doi.org/10.1016/j.jim.2005.05.005.

Ito, H., Wate, R., Zhang, J., Ohnishi, S., Kaneko, S., Ito, H., Nakano, S., Kusaka, H., 2008. Treatment with edaravone, initiated at symptom onset, slows motor decline and decreases SOD1 deposition in ALS mice. Exp. Neurol. 213 (2), 448–455. https://doi.org/10.1016/j.expneurol.2008.07.017.

Jaiswal, M.K., 2018. Riluzole and edaravone: a tale of two amyotrophic lateral sclerosis drugs. Med. Res. Rev. 39 (2), 733–748. https://doi.org/10.1002/med.21528.

Krock, E., Millecamps, M., Anderson, K.M., Srivastava, A., Reihsen, T.E., Hari, P., Sun, Y. R., Jang, S.H., Wilcox, G.L., Belani, K.G., Beebe, D.S., Ouellet, J., Pinto, M.R., Kehl, L. J., Haglund, L., Stone, L.S., 2019. Interleukin-8 as a therapeutic target for chronic low back pain: upregulation in human cerebrospinal fluid and pre-clinical validation with chronic reparixin in the SPARC-null mouse model. EBioMedicine 43, 487–500. https://doi.org/10.1016/j.ebiom.2019.04.032.

La Cognata, V., Gentile, G., Aronica, E., Cavallaro, S., 2020. Splicing players are differently expressed in sporadic amyotrophic lateral sclerosis molecular clusters and brain regions. Cells 9 (1). https://doi.org/10.3390/cells9010159.

Lederer, C.W., Torrisi, A., Pantelidou, M., Santama, N., Cavallaro, S., 2007. Pathways and genes differentially expressed in the motor cortex of patients with sporadic amyotrophic lateral sclerosis. BMC Genomics 8, 26. https://doi.org/10.1186/1471-2164-8-26.

Lippert, U., Zachmann, K., Henz, B.M., Neumann, C., 2004. Human T lymphocytes and mast cells differentially express and regulate extra- and intracellular CXCR1 and CXCR2. Exp. Dermatol. 13 (8), 520–525. https://doi.org/10.1111/j.0906-6705.2004.00182.x.

Mandillo, S., Tucci, V., Holter, S.M., Meziane, H., Banchaabouchi, M.A., Kallnik, M., Lad, H.V., Nolan, P.M., Ouagazzal, A.M., Coghill, E.L., Gale, K., Golini, E., Jacquot, S., Krezel, W., Parker, A., Riet, F., Schneider, I., Marazziti, D., Auwerx, J., Brown, S.D., Chambon, P., Rosenthal, N., Tocchini-Valentini, G., Wurst, W., 2008. Reliability, robustness, and reproducibility in mouse behavioral phenotyping: a cross-laboratory study. Physiol. Genomics 34 (3), 243–255 doi: 90207.2008 [pii]. https://doi.org/10.1152/physiolgenomics.90207.2008.

Marsh, D.R., Flemming, J.M., 2011. Inhibition of CXCR1 and CXCR2 chemokine receptors attenuates acute inflammation, preserves gray matter and diminishes autonomic dysreflexia after spinal cord injury. Spinal Cord 49 (3), 337–344. https://doi.org/10.1038/sc.2010.127.

Mathis, S., Goizet, C., Soulages, A., Vallat, J.-M., Masson, G.L., 2019. Genetics of amyotrophic lateral sclerosis: a review. J. Neurol. Sci. 399, 217–226. https://doi.org/10.1016/j.jns.2019.02.030.

Matsushita, H., Hijioka, M., Ishibashi, H., Anan, J., Kurauchi, Y., Hisatsune, A., Seki, T., Shudo, K., Katsuki, H., 2014. Suppression of CXCL2 upregulation underlies the therapeutic effect of the retinoid Am80 on intracerebral hemorrhage in mice. J. Neurosci. Res. 92 (8), 1024–1034. https://doi.org/10.1002/jnr.23379.

Melanie Leitner, S.M., Lutz, Cathleen, 2009. Working with ALS Mice - Guidelines for Preclinical Testing & Colony Management. Prize-4Life and The Jackson Laboratory, pp. 1–21.

Morello, G., Cavallaro, S., 2015. Transcriptional analysis reveals distinct subtypes in amyotrophic lateral sclerosis: implications for personalized therapy. Future Med. Chem. 7 (10), 1335–1359. https://doi.org/10.4155/fmc.15.60.

Morello, G., Conforti, F.L., Parenti, R., D'Agata, V., Cavallaro, S., 2015. Selection of potential pharmacological targets in ALS based on whole- genome expression profiling. Curr. Med. Chem. 22 (17), 2004–2021.

Morello, G., Spampinato, A.G., Cavallaro, S., 2017a. Molecular taxonomy of sporadic amyotrophic lateral sclerosis using disease-associated genes. Front. Neurol. 8, 152. https://doi.org/10.3389/fneur.2017.00152.

Morello, G., Spampinato, A.G., Cavallaro, S., 2017b. Neuroinflammation and ALS: transcriptomic insights into molecular disease mechanisms and therapeutic targets. Mediat. Inflamm. 2017, 7070469. https://doi.org/10.1155/2017/7070469.

Morello, G., Spampinato, A.G., Conforti, F.L., D'Agata, V., Cavallaro, S., 2017c. Selection and prioritization of candidate drug targets for amyotrophic lateral sclerosis through a meta-analysis approach. J. Mol. Neurosci. 61 (4), 563–580. https://doi.org/10.1007/s12031-017-0898-9.

Morello, G., Guarnaccia, M., Spampinato, A.G., La Cognata, V., D'Agata, V., Cavallaro, S., 2018. Copy number variations in amyotrophic lateral sclerosis: piecing the mosaic tiles together through a systems biology approach. Mol. Neurobiol. 55 (2), 1299–1322. https://doi.org/10.1007/s12035-017-0393-x.

Morello, G., Guarnaccia, M., Spampinato, A.G., Salomone, S., D'Agata, V., Conforti, F.L., Aronica, E., Cavallaro, S., 2019. Integrative multi-omic analysis identifies new drivers and pathways in molecularly distinct subtypes of ALS. Sci. Rep. 9 (1), 9968. https://doi.org/10.1038/s41598-019-46355-w.

Morello, G., Salomone, S., D'Agata, V., Conforti, F.L., Cavallaro, S., 2020. From multi-omics approaches to precision medicine in amyotrophic lateral sclerosis. Front. Neurosci. 14, 577755 https://doi.org/10.3389/fnins.2020.577755.

Nguyen, D., Stangel, M., 2001. Expression of the chemokine receptors CXCR1 and CXCR2 in rat oligodendroglial cells. Brain Res. Dev. Brain Res. 128 (1), 77–81.
Nilsson, G., Mikovits, J.A., Metcalfe, D.D., Taub, D.D., 1999. Mast cell migratory response to Interleukin-8 is mediated through interaction with chemokine receptor CXCR2/interleukin-8RB. Blood 93 (9), 2791–2797. https://doi.org/10.1182/blood.V93.9.2791.
Nirodi, C.S., Devalaraja, R., Nanney, L.B., Arrindell, S., Russell, S., Trupin, J., Richmond, A., 2008. Chemokine and chemokine receptor expression in keloid and normal fibroblasts. Wound Repair Regen. 8 (5), 371–382. https://doi.org/10.1111/j.1524-475X.2000.00371.x.
Oliván, S., Calvo, A.C., Manzano, R., Zaragoza, P., Osta, R., 2014. Sex differences in constitutive autophagy. Biomed. Res. Int. 2014, 1–5. https://doi.org/10.1155/2014/652817.
OlivÁN, S., Calvo, A.C., Rando, A., MuÑOz, M.J., Zaragoza, P., Osta, R., 2015. Comparative study of behavioural tests in the SOD1G93A mouse model of amyotrophic lateral sclerosis. Exp. Anim. 64 (2), 147–153. https://doi.org/10.1538/expanim.14-0077.
Popivanova, B.K., Koike, K., Tonchev, A.B., Ishida, Y., Kondo, T., Ogawa, S., Mukaida, N., Inoue, M., Yamashima, T., 2003. Accumulation of microglial cells expressing ELR motif-positive CXC chemokines and their receptor CXCR2 in monkey hippocampus after ischemia-reperfusion. Brain Res. 970 (1–2), 195–204. https://doi.org/10.1016/s0006-8993(03)02343-6.
Raoul, C., Li, J., Sung, M., Rutkove, S.B., 2013. Electrophysiologic biomarkers for assessing disease progression and the effect of Riluzole in SOD1 G93A ALS mice. PLoS One 8 (6), e65976. https://doi.org/10.1371/journal.pone.0065976.
Semple, B.D., Kossmann, T., Morganti-Kossmann, M.C., 2010. Role of chemokines in CNS health and pathology: a focus on the CCL2/CCR2 and CXCL8/CXCR2 networks. J. Cereb. Blood Flow Metab. 30 (3), 459–473. https://doi.org/10.1038/jcbfm.2009.240.
Sousa, L.F., Coelho, F.M., Rodrigues, D.H., Campos, A.C., Barcelos Lda, S., Teixeira, M. M., Rachid, M.A., Teixeira, A.L., 2013. Blockade of CXCR1/2 chemokine receptors protects against brain damage in ischemic stroke in mice. Clinics (Sao Paulo) 68 (3), 391–394. https://doi.org/10.6061/clinics/2013(03)oa17.
Strieter, R.M., Polverini, P.J., Arenberg, D.A., Kunkel, S.L., 1995. The role of cxc chemokines as regulators of angiogenesis. Shock 4 (3), 155–160. https://doi.org/10.1097/00024382-199509000-00001.
Taylor, S.C., Nadeau, K., Abbasi, M., Lachance, C., Nguyen, M., Fenrich, J., 2019. The ultimate qPCR experiment: producing publication quality, reproducible data the first time. Trends Biotechnol. 37 (7), 761–774. https://doi.org/10.1016/j.tibtech.2018.12.002.
Turner, M.R., Parton, M.J., Leigh, P.N., 2001. Clinical trials in ALS: an overview. Semin. Neurol. 21 (2), 167–175. https://doi.org/10.1055/s-2001-15262.
van Es, M.A., Hardiman, O., Chio, A., Al-Chalabi, A., Pasterkamp, R.J., Veldink, J.H., van den Berg, L.H., 2017. Amyotrophic lateral sclerosis. Lancet 390 (10107), 2084–2098. https://doi.org/10.1016/s0140-6736(17)31287-4.
Veenstra, M., Ransohoff, R.M., 2012. Chemokine receptor CXCR2: physiology regulator and neuroinflammation controller? J. Neuroimmunol. 246 (1–2), 1–9. https://doi.org/10.1016/j.jneuroim.2012.02.016.
Villa, P., Triulzi, S., Cavalieri, B., Di Bitondo, R., Bertini, R., Barbera, S., Bigini, P., Mennini, T., Gelosa, P., Tremoli, E., Sironi, L., Ghezzi, P., 2007. The interleukin-8 (IL-8/CXCL8) receptor inhibitor reparixin improves neurological deficits and reduces long-term inflammation in permanent and transient cerebral ischemia in rats. Mol. Med. 13 (3–4), 125–133. https://doi.org/10.2119/2007-00008.Villa.
Walz, A., Peveri, P., Aschauer, H., Baggiolini, M., 1987. Purification and amino acid sequencing of NAF, a novel neutrophil-activating factor produced by monocytes. Biochem. Biophys. Res. Commun. 149 (2), 755–761. https://doi.org/10.1016/0006-291x(87)90432-3.
Weydt, P., Hong, S.Y., Kliot, M., Möller, T., 2003. Assessing disease onset and progression in the SOD1 mouse model of ALS. NeuroReport 14 (7), 1051–1054. https://doi.org/10.1097/01.wnr.0000073685.00308.89.
Won, Y.H., Lee, M.Y., Choi, Y.C., Ha, Y., Kim, H., Kim, D.Y., Kim, M.S., Yu, J.H., Seo, J. H., Kim, M., Cho, S.R., Kang, S.W., 2016. Elucidation of relevant Neuroinflammation mechanisms using gene expression profiling in patients with amyotrophic lateral sclerosis. PLoS One 11 (11), e0165290. https://doi.org/10.1371/journal.pone.0165290.